



Earthquake and rainfall-induced landslide hazard assessment of Kutupalong Rohingya camp using meteorological and geological information

Anika Samm-A¹ · A. S. M. Maksud Kamal¹ · Md. Zillur Rahman¹

Accepted: 22 February 2023 / Published online: 10 March 2023

© The Author(s), under exclusive licence to Springer-Verlag GmbH Germany, part of Springer Nature 2023

Abstract

Kutupalong Rohingya camp is one of the largest humanitarian shelters for conflict-fled people. The camp area is susceptible to landslide hazards because of being situated in dynamic tectonic settings and meteorological conditions. Hence, the study aims to assess the earthquake and rainfall-induced landslide hazards in the camp for the worst-case scenario. The landslide triggering parameters (topographic, soil physical property, and contributing factors) are designed in the study to identify the hazard-prone areas through the factor of safety computation. The topographic parameters are prepared by combining field investigation and remote sensing-based information. The soil physical properties are modeled in two ways to account for their uncertainties: normal probabilistic distribution and interpolation-based spatial distribution. The contributing factors (i.e., earthquake and rainfall) have been assessed using the probabilistic approach. The Peak Ground Acceleration (PGA) exceedance of 50, 75, 100, 200, and 475 years return periods are applied in the factor of safety calculation for earthquake-induced landslides. The rainfall intensities of 50 and 75 years return periods are combined with the PGA exceedance of the respective years to assess the earthquake and rainfall-triggered landslide-prone areas. The factor of safety has been measured following two methods: Monte-Carlo simulation and direct estimation method. Multiple scenarios (rainfall with the duration of 1, 2, and 3 days) are also considered to estimate the landslide-prone areas in these models. The study findings are finally validated against field investigation-based landslide inventory with more than 85% accuracy at a 90% confidence interval.

Keywords Earthquake and rainfall · Monte-Carlo simulation · Landslides · Factor of safety

1 Introduction

Landslide is a common hazard in mountainous areas having severe impacts. Owing to a lack of standard accommodation facilities, people often need to live under or on the slope of the hills, which bears fatal consequences. Both rainfall (intense and prolonged) and earthquakes can trigger landslide events in those areas (Terzaghi and Voight 1979). Southeast mountainous region of Bangladesh experiences heavy rainfall during the monsoon, and due to the country's tectonic settings, it is prone to earthquake

hazards as well (Kamal 2013). These two conditions make the region more susceptible to landslides. Over the last two decades, more than 400 people have died, and 56,000 people have been affected by landslides in this region (Chisty 2014). Unfortunately, this region provides shelter to Myanmar's conflict-fled population of Rohingya. The Kutupalong Rohingya camp, providing shelter to these people since 1991 (informally), is situated in this landslide-prone region. The camp of a total 13km² area, provides shelter to almost 913,660 people (30 November 2021; UNHCR 2021). Though situated in an almost mountainous region, the camp's significant proportion of hills has been cut into plain areas to fulfill the settlement demand of the enormous influx of Rohingyas. While setting up their residence, these people contribute to landslide hazards. The camp has some previous cases of striking landslides with casualties and damages. For four consecutive years (i.e.,

✉ A. S. M. Maksud Kamal
maksudkamal@du.ac.bd

¹ Department of Disaster Science and Climate Resilience,
University of Dhaka, Dhaka 1000, Bangladesh

2018, 2019, 2020, and 2021), there has been news of landslide occurrence and even casualties in the camp (ISCG 2018; Reliefweb 2019; Aziz 2021; Giiespie 2021). Upon sudden arrival in 2017, the Rohingyas indiscriminately cut the slopes and trees to establish their makeshift houses at the camp, triggering the landslide event. When the first monsoon hit in 2018 after their arrival, neither the Rohingyas nor the management was prepared for this extreme event (Reliefweb 2018). In the later years, the camp repeatedly underwent and is still undergoing this disastrous hazard.

The camp lies in a region where tectonic activities are prominent due to the presence of the Indo-Burman region (Wang et al. 2014). This area lies within the seismic Zone-III according to the Bangladesh National Building Code (BNBC 2020). Several noteworthy earthquakes have occurred within the 300 km radius of the camp, and their shaking has also been experienced in the campsite (Wang et al. 2014; Wang and Kerry 2013). In monsoon, the camp experiences prolonged intensified rainfall just like the rest of the country, mainly in June–July month. The closest meteorological station (Teknaf) in this area has the highest rainfall intensity record of 481 mm/day in the last 10 years (BMD 2021). With rainfall incidents, the pore water pressure within the soil increases and shear strength decreases. Slope failure occurs, resulting in landslides which are locally termed “Handya”. During these rainfall-influenced times, there remains the possibility of earthquake occurrence. Owing to the chances of being exposed to earthquakes and rainfall simultaneously or sequentially, the camp may face the worst-case scenarios of landslides. These events should be assessed urgently since the camp population is already fighting with identity, nationality, shelter, food, standard health, nutrition, education, and sanitary crises. For the management to be better prepared and equipped, landslide-prone areas of the camp should be identified. Hence, landslide assessment has been carried out for the camp so that the findings of the study may contribute to the response, rehabilitation, and mitigation activities encouraging safer settlement of this large community (Fig. 1).

The earliest attempt to evaluate the stability of any slope against failure caused by earthquake is the pseudo-static factor of safety analysis. This method considers earthquake loading as a static horizontal force in the static limit equilibrium method. This method is first documented by Terzaghi (1950) for earthen dams. Terzaghi and Voight (1979) explained the impact of pore water pressure on rocks and their resultant landslides. Later, Seed (1979) updated Terzaghi’s (1950) basic equation and accounted for the uncertainties. Marcuson (1981) examined the stability of dams and slopes for dynamic loads. Intensity–duration–frequency (IDF) relation became a popular

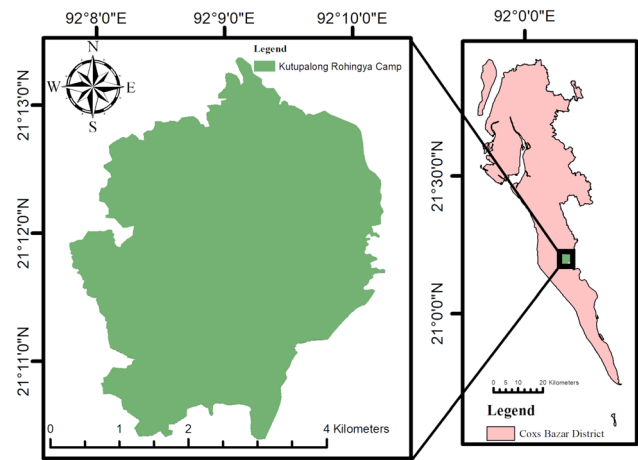


Fig. 1 Kutupalong Rohingya Camp, situated at the Cox’s Bazar District

approach (2000–2021) to assess landslides induced by rainfall (Aristizábal et al. 2020; Borga et al. 2002; Hossain and Toll 2020). Du and Wang (2014) introduced the Monte-Carlo simulation technique for seismic displacement analysis. Haneberg (2004) adopted an uncertainty model for input parameters to compute the factor of safety. Jibson (2011) considered gravity and seismic loads for static limit equilibrium analysis to assess landslides.

The pseudo-static analysis considers an earthquake as a permanent unidirectional force causing slope instability. Earthquake coefficients are incorporated to compensate for this unidirectional conservative instability approach due to the brief shorter effect of PGA on sliding mass (Hynes Griffin and Franklin 1984; Marcuson 1981). The selection of seismic coefficients is quite a challenging task. However, according to Kramer (1996), there is flexibility in selecting the value of seismic coefficients. The number of assessment studies on both earthquake and rainfall-induced landslides can be scarcely found. Nguyen and Kim (2020) assessed landslide hazards on mount Umeyon in South Korea using the Monte-Carlo simulation technique, where the parameters were considered normally distributed. They incorporated both earthquake and rainfall as triggering factors and modeled the landslide-prone areas. However, the effects of rainfall duration remained mostly under-attended in their work.

Several studies have been conducted to assess landslide hazards in the camp and host community area. Ahmed (2015) applied user-defined weighting and data-driven statistical techniques in Cox’s Bazar Municipality, known as the host community to model landslide susceptibility. Haque et al. (2018) identified landslide-prone areas within the camp through high-resolution DEM and SAR offset tracking techniques. Tehrani and Hüsken (2019) used 12 controlling factor and frequency ratio maps to produce a susceptibility map of the refugee camp. Elsewhere, Ahmed

et al. (2020) combined rainfall thresholds, landslide susceptibility, and inventory maps to produce a localized Early Warning System (EWS) for the host community and the camp itself. In most cases, the studies mainly focused on rainfall as the triggering event. The simultaneous or sequential occurrence of rainfall and earthquake has not been adequately considered in them. Thus, the extreme case scenario has not been addressed yet. Besides, the uncertainties associated with the soil physical parameters should be dealt with caution as it is practically difficult to design these parameters only from field observation. Therefore, this study considers both earthquake and rainfall as contributing factors, taking into account the rainfall duration. It designs the physical property parameters with Monte-Carlo simulation and IDW interpolation and finds the landslide-prone areas through Monte-Carlo simulation and direct calculation which also includes comparing their results. Monte Carlo simulation has been chosen for the study to address the uncertainty issue regarding the physical property parameters. The simulation considers random values from any probabilistic distribution rather than grabbing one specific value. Using this simulation, the study has dealt with the uncertainty of soil physical property parameters.

2 Materials and method

This study is designed considering three types of parameters mainly: topographic parameters, soil physical property parameters, and contributing factors. These parameters were applied to the final static limit equilibrium analysis to find the factor of safety (Fig. 2).

2.1 Topographic parameters

The slope of the study area is considered one of the most crucial parameters for landslide hazards. It is an indicator of surface characteristics (Seda 2020). Slopes can be collected utilizing the Digital Elevation Model (DEM). This study has used 0.5×0.5 m resolution DEM to calculate the slope of the camp area. The DEM is obtained from Inter-Agency Coordination Group (IACG), IOM. The DEM was prepared using a UAV in 2019. The DEM is validated against the Survey of Bangladesh (SoB) data before its use. The calculated Root Mean Square Error was 1.57. Slope values were obtained for the study area using ArcMap spatial analyst tool. The slope value ranged from 0° to 86° . Around 65% of the area has a slope value lower than 20° (Fig. 3a).

The curvature parameter depicts the shape of the surface. It is computed through the second derivative of the surface. The curvature value can be understood from the drainage pattern, soil erosion pattern, water distribution on

land, convergence or divergence, and acceleration or deceleration of the flow (ESRI 2021). The curvature of the study area was obtained from the DEM of 2019. Steep mountainous areas tend to have a -5 to 5 value for curvature. However, the hilly area ranges from -0.5 to 0.5 . Curvature value ranges from -5 to 7 for the study area (Fig. 3b) among which 70% of the area has curvature values ranging from -0.5 to 0.5 . The curvature value is affected due to the significant anthropogenic influences on the camp area.

Soil depth is another important parameter for assessing landslide hazards. The soil depth of the study area was obtained by combining field observation and the soil depth model of Saulnier et al. (1997), shown in Eq. 1. This model allows spatial variability with soil depth and considers the maximum-minimum soil depth and elevation value. The DEM has fed the elevation data for the study area. Maximum and minimum soil depths were obtained from the field investigation. For the study area, soil depth value ranges from 0 to 5 m (Fig. 3c).

$$\text{Soil depth, } H_{\text{pixel } i} = D_{\text{max}} - \frac{Z_{\text{pixel } i} - Z_{\text{min}}}{Z_{\text{max}} - Z_{\text{min}}} (D_{\text{max}} - D_{\text{min}}) \quad (1)$$

Here, *Soil depth*, $H_{\text{pixel } i}$ (m) is the depth of soil for *i*th pixel; $Z_{\text{pixel } i}$ (m), Z_{min} (m) and Z_{max} (m) are the *i*th pixel, minimum and maximum elevation values of DEM, respectively. D_{max} (m) and D_{min} (m) are the maximum and minimum soil depths obtained from field observation.

2.2 Soil physical property parameters

Soil's physical properties are equally crucial while analyzing landslide hazards. The geological and geotechnical features of the study area define the hazard pattern. Soil physical property parameters do not hold a single value throughout the study area. Two different approaches are applied to compensate for the spatial variability of these parameters.

The first one considers them normally distributed with their mean and standard deviation. Monte-Carlo simulation has been used in the study to support the probabilistic approach. This specific method was used because it models the output of different combinations more efficiently when the predictions are quite challenging due to random variable hindrance. During the computation, a random value of the soil physical property parameters was taken from their respective normal distribution for each MC run ($N = 1000$). Finally, the average value was obtained. The study has run the simulations 1000 times as after 1000 runs, the difference in standard deviation tends to be 0 for all the 0.1, 0.5, 1, and 5 standard deviation value scenarios (Fig. 4).

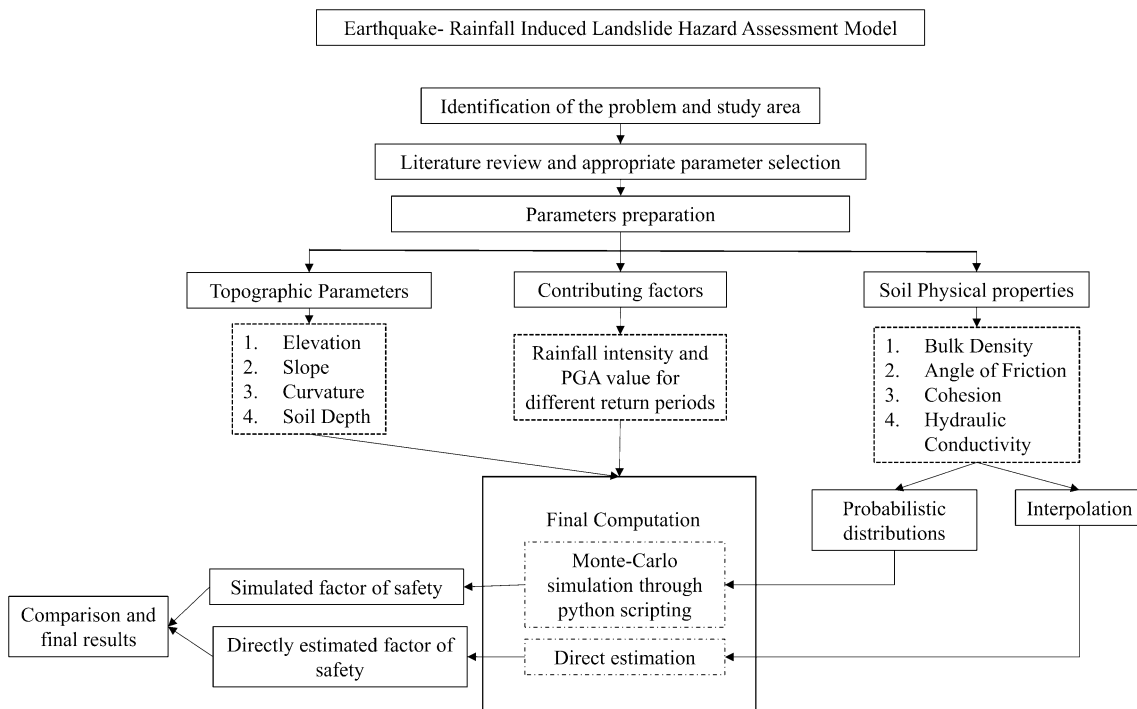


Fig. 2 Methodological framework of the study

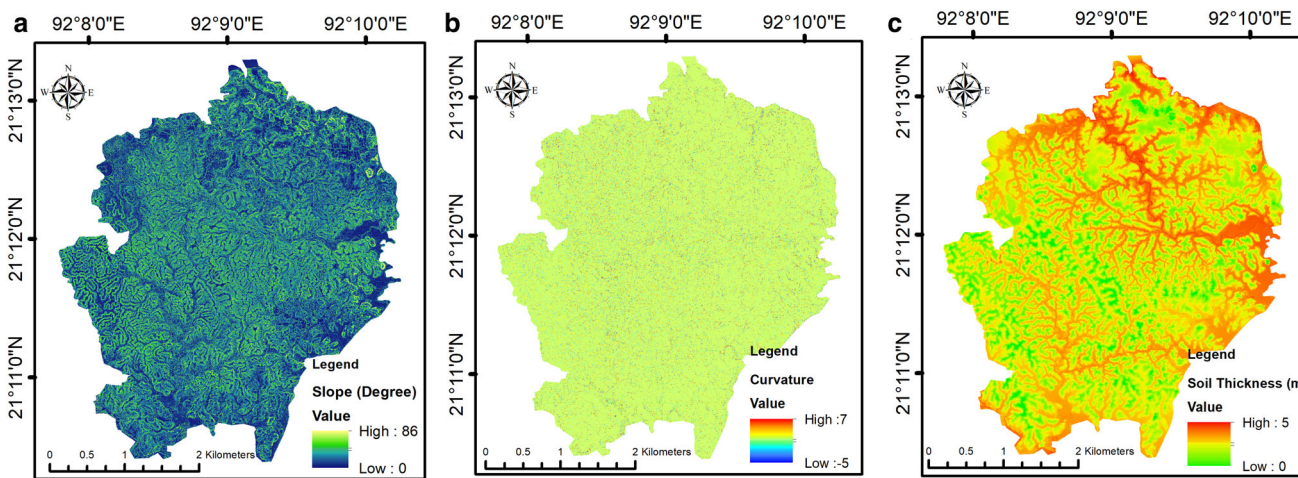


Fig. 3 Topographic parameters used in the study. a the map of slope in degree unit. b the curvature. c the soil thickness in meter unit

Another approach is the interpolation one. Physical property parameters are obtained from field observation and lab tests. The lab tests have followed the American Society of Testing Materials (ASTM) specified procedures. The entire study area was mapped utilizing the samples collected from field surveys at specific points. For mapping, the IDW interpolation mechanism was adopted.

Soil physical property parameters obtained from these two approaches are later applied separately in the final factor of safety calculation, and their results are compared.

Unit weight, Friction angle, and Cohesion have been directly assessed from lab tests. Hydraulic Conductivity has been calculated from the Grain Size Distribution (GSD) data. Unit weight, the component of soil, is the ratio of total weight to its total volume. The unit weight is obtained for soil samples through the ratio of total soil weight to its total volume collected in a brass ring. Soil samples have been collected from 36 points throughout the study area, and their bulk density and unit weight have been measured. The average value and the standard deviation of the entire study area have been calculated from

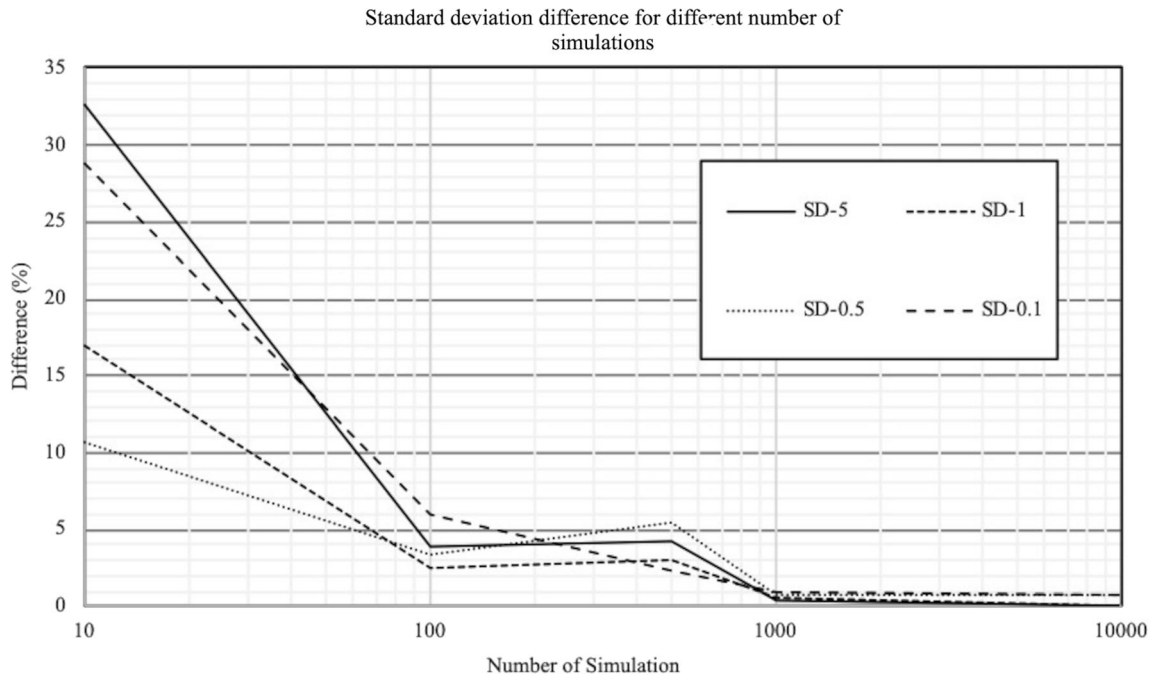


Fig. 4 Estimation of minimum number of Monte-Carlo simulation (standard deviation differences for different number of simulations)

Table 1 Soil physical property parameter values used in Monte-Carlo simulation

Parameter name	Mean value	Standard deviation	Source
Bulk density (kg/m ³)	17.14	1.45	Field data and laboratory test (ASTM)
Cohesion (KN/m ²)	6.37	3.81	Field data and laboratory test (ASTM)
Friction angle (°)	35.69	1.67	Field data and laboratory test (ASTM)
Hydraulic conductivity (mm/h)	0.211	0.14	Field data and laboratory test; modeled from GSD

these 36 locations’ data for Monte- Carlo simulation model (Table 1). IDW interpolation has been run on the study area for the direct estimation model based on these 36 lab-tested samples (Fig. 5a).

The angle of friction provides an idea of the shear resistance of the soil sample. Preliminary Grain Size Distribution (GSD), particle interlocking, and angularity reshape friction angle specifying the inclination of the failure envelope in a Mohr’s Circle. Coarse-grained angular sands have a greater angle of friction than finer-grained rounded sands (Factor Geotechnical 2021). Soil samples have been collected at 36 points from field investigation, and their angle of friction is estimated. From these points, mean and standard deviations are obtained for the Monte-Carlo simulation (Table 1). A spatial distribution model has been prepared using IDW interpolation for the direct estimation model (Fig. 5b). Cohesion is another shear strength parameter that binds soil particles together. Finer grain soils tend to have higher cohesion values. The same approaches were undertaken to design the cohesion parameter as unit weight and angle of friction (Fig. 5c).

Hydraulic conductivity is essential for assessing the hydraulic characteristics of any geological unit. It is mainly used to measure flow velocity. The study assessed hydraulic conductivity to determine the flow velocity, later used in the factor of safety calculation equation. Hydraulic conductivity in the study was estimated from Grain Size Distribution data. Grain Size distribution was assessed in the lab tests following ASTM standards. Later, using the effective size (d_{10}), hydraulic conductivity was estimated with the empirical equation from Wang et al. (2017):

$$K = C_H \frac{g}{\nu} d_{10}^2 \tag{2}$$

Here, g denotes the gravitational acceleration (m/s²), C_H represents a unitless coefficient whose value is around 6.54×10^{-4} (Harleman et al. 1963), and ν is the kinetic viscosity for water (0.89×10^{-6} m²/s at 25 °C).

From field investigation, it is apparent that the study area has brown to yellowish moderately hard to loose sandstones with insignificant amounts of clay and shale. The amount of clay and shale found in the study area is not

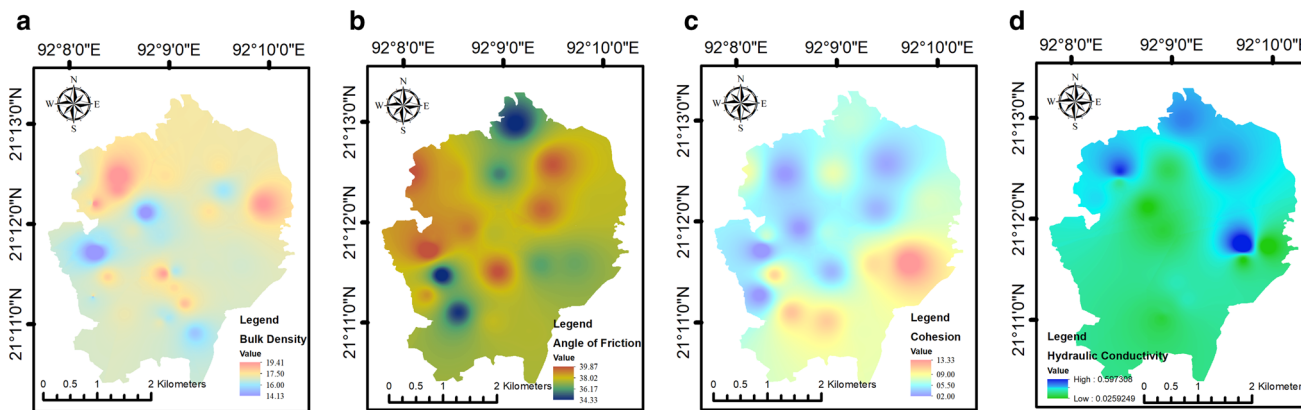


Fig. 5 The soil physical property parameters (interpolated maps) used in direct estimation method. **a** The bulk density in kg/m³ unit, **b** the angle of friction in degree unit, **c** cohesion in KN/m² unit and **d** hydraulic conductivity in mm/h unit

enough to claim the presence of Girujan clay. Moreover, the study area lies north of the Teknaf peninsula on a bathtub-like syncline (McClymont et al. 2017). The dip angles of the beds are also relatively small, closer to 0°–10°. Therefore, the entire study area is considered to have Dupi Tila formation. The values (mean and Standard deviation) of all the soil physical properties parameters are considered constant for the entire study area of the Monte-Carlo simulation model.

2.3 Contributing factors

2.3.1 Rainfall intensity

The annual probability of exceedance of rainfall intensity (mm/day) is calculated from 2000 to 2019 daily rainfall data. They are collected from Bangladesh Meteorological Department (BMD) for the Teknaf station (BMD 2021). The maximum intensity of rainfall per day for each year is considered for the computation (considering the worst-case scenario). The maximum rainfall intensity for these 20 years varies from the lowest 135 mm/day (in 2002) to the highest 481 mm/day (in 2010). The average amount of time it takes for any severe event of a certain size or magnitude to be equaled or exceeded at least once is known as the return period or recurrence interval. It is a common practice to assess the exceedance probability of rainfall using a plotting position formula (an empirical one). Our study has used Weibull’s Plotting Position formula (Chow 1964). This formula is widely used as it is better at achieving unbiased exceedance probabilities (Cunnane 1978). This plot is obtained arranging the rainfall data in descending order attributing their respective rank as

$$T = \frac{N + 1}{R} \tag{3}$$

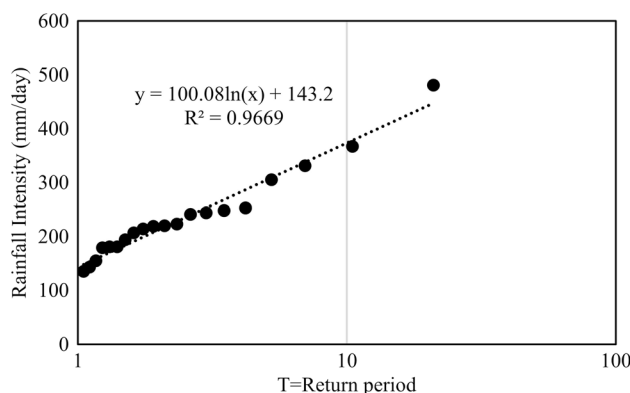


Fig. 6 Weibull’s Plot for assessing rainfall intensity for 50 and 75 years return period

Table 2 Rainfall intensity and PGA values used in the study for different return periods

Return period (Years)	Rainfall intensity (mm/day)	PGA (g) exceedance
50	534	0.039
75	575	0.066
100	–	0.085
200	–	0.140
475	–	0.230

where *T* is the return period, *N* represents the total number of years of record and *R* denotes the rank of rainfall intensities organized in descending order (Fig. 6).

Using the plot, rainfall intensity for specific return periods like 50 and 75 years were assessed and considered later for final computation (Table 2).

2.3.2 Peak ground acceleration (PGA) values for earthquake

At bedrock conditions, the hazard values in peak ground acceleration (PGA) were computed for the 50, 75, 100, 200, and 475 years return period for the study area. A probabilistic approach has been taken to assess the seismic hazard. Possible source models, Possible GMPE combinations were used with the logic tree combination approach.

This study utilized an updated combined earthquake source model (background seismicity, linear, and areal source models) and two sets of ground motion prediction equations through the standard logic tree structure to minimize the epistemic uncertainty in hazard calculation.

In Background seismicity, adjacent areas within 300 km of the study area were divided into 0.1×0.1 degree grid points. The smoothed seismicity rate, Gutenberg–Richter b value, and maximum magnitude were calculated. The b value computed for the background seismicity model equals 0.85. This is the regional b value of declustered catalog.

Twenty linear sources (both known slip and unknown slip types) were considered for the linear source model. The known slip type linear sources are Dauki, Dapsi, Dhubri, Oldham, Kopili, Kabaw, Churachandpur Mao, and Laymyo. The unknown slip type linear sources are Saintmartin, Dakshin Nila, Maheshkhali, Jaldi, Patiya, Sitakund, Lalmai, Habiganj, Rashidpur, Sylhet, and Fenchuganj. For the unknown slip type linear sources, the possibility of two types of slip mechanisms (reverse and strike slip) was considered, giving them equal weights. Their recurrence parameters were assessed using both the characteristic and Gutenberg–Richter models. Maximum magnitude was estimated using the empirical scaling relationships of magnitude and rupture characteristics of Wells and Coppersmith (1994) and Blaser et al. (2010). They were given equal weight in logic tree approach.

Ten areal source zones were delineated for this study. They were based on the changes of seismicity in case of magnitude and focal depth distributed in the study area, consideration of events in the comprehensive declustered catalog around geological structures, and published literature dealing with a concept similar to this study. The sources are the Himalayan zone, Dauki-Shillong plateau, Naga interface and intraslab sections, Chittagong-Tripura fold belt, Ramree section and its extension, partial Sagaing section, and stable continental crust. Their seismicity parameters (seismicity rate, Gutenberg–Richter b value, and maximum magnitude) were also assessed.

Finally, seismic hazard was assessed applying two suitable GMPE sets (shallow crustal zone GMPEs and subduction zone GMPEs) with justifiable weightings, using the logic tree approach for all three types of sources as well

as combining them. The PGA values for 50, 75, 100, 200, and 475 years return periods are later used in the final computation.

2.4 Hazard calculation

Final computation has been carried out by preparing all the topographic parameters, soil physical properties, and contributing factors (earthquake and rainfall). Two types of computation have been completed. 1. Monte Carlo simulation and 2. Direct computation. These approaches are considered useful to address the uncertainties regarding the spatial distribution of soil physical properties parameters. Both the calculations are run on the updated pseudo-static factor of safety estimation equation of Terzaghi (1950).

$$FS_{ps} = \frac{c + [(\gamma H - \gamma_w h) \cos^2 \alpha] \tan \phi - k \gamma H \sin \alpha \cdot \cos \alpha \cdot \tan \phi}{\gamma H \sin \alpha \cos \alpha + k \gamma H \cos^2 \alpha} \quad (4)$$

$$k = 0.5 \frac{\text{PGA}}{g} \quad (5)$$

Here, γ denotes the unit weight of soil (kN/m^3), H denotes the depth of soil (m), γ_w denotes the unit weight of water (kN/m^3), h denotes the saturated depth (m), ϕ denotes the angle of friction (o), α denotes the slope angle, c denotes the cohesion (kN/m^2), k denotes earthquake coefficients, PGA (m/s^2) denotes the peak ground acceleration of an earthquake, and g denotes the acceleration due to gravity (m/s^2).

The pseudo-static factor of safety is influenced mainly by the earthquake coefficients (combination of a constant value and PGA value). Earthquake coefficients can vary from 0.1 to 0.5. Several authors have proposed different k values for different PGAs (e.g., Hynes Griffin and Franklin 1984; Seed 1979; Zhang 2015). This study considered k values (0.1–0.5) at different PGAs and compared their outputs. Lower and greater values of k show fewer deviations for both the lower PGA values; higher values of k show more significant variations of the factor of safety at higher PGAs. The factor of safety tends to decrease significantly at higher PGA values. As the study aims to assess the landslide hazard in the worst-case scenario, 0.5 has been considered for final computation.

Saturated depth was used to incorporate the influence of rainfall, which mainly depends on rainfall intensity, curvature value, and rainfall duration. Iida (1984) has proposed a steady-state hydrological model for saturated depth estimation.

$$h = \frac{R_I}{n} \left[t + \left(\frac{e}{2} \right) V_s t^2 \right] \quad (6)$$

$$V_s = \frac{k_s}{n} \sin \alpha \cos \alpha \quad (7)$$

where RI is the intensity of precipitation (rainfall), ε is the curvature for specific terrain cell (m^{-1}), t is the rainfall duration in days, V_s is the bedrock parallel flow's horizontal velocity component (m/day), and n is the effective porosity.

Monte Carlo simulation mainly works on repeated random sampling algorithms for mathematical computation. Monte-Carlo simulation is beneficial for those data generation methods which have several constraints. Soil physical properties are modeled with Monte-Carlo simulation. They are considered normally distributed. Therefore, 1000 simulations were run during the final computation where Eq. 3 picked a value from the normal distribution of the soil physical property parameters and calculated the respective safety factor. The final factor of safety was obtained from these 1000 simulations. Since the parameters are designed in probabilistic distribution, the factor of safety is obtained through a probabilistic approach to reduce the uncertainty of spatial variability.

In the direct estimation, the same equation was applied. Spatially variable soil physical parameters obtained from the IDW interpolations were used for this computation. The results were directly obtained without multiple times simulations. Finally, the pixel values with the factor of safety value less than one were taken as landslide-prone from the computation.

3 Result

After final computation, landslide-prone areas of the Kutupalong Rohingya Camp were identified following the Monte-Carlo simulation and direct estimation methods. The study has considered different PGA values and rainfall intensity combinations for different return periods (50 and 75 years). In addition, it attempted to assess the effect of specific rainfalls at a prolonged intensity of 1, 2 and 3 days on landslide hazards in the local area. Reviewing the 20 years of data on rainfall intensity for Teknaf station, it is evident that similar intensity of rainfall (± 5 mm) can sustain for 2 or 3 days (Fig. 7). Therefore, the study has considered the same rainfall intensity for 1, 2 and 3 days for the respective return periods (50 and 75 years). The study uses only 20 years of rainfall data record. It considers rainfall intensity up to 75 years return period for the factor of safety computation. It would not be wise to project rainfall intensity for more than 75 years return period based on only 20 years of data (the influence of climate change may also be present). Hence, the combined impact of rainfall and earthquake has been considered for 50 and 75 years to compute the factor of safety.

However, earthquake PGAs for more than 75 years return period are significant. Therefore, landslide-prone

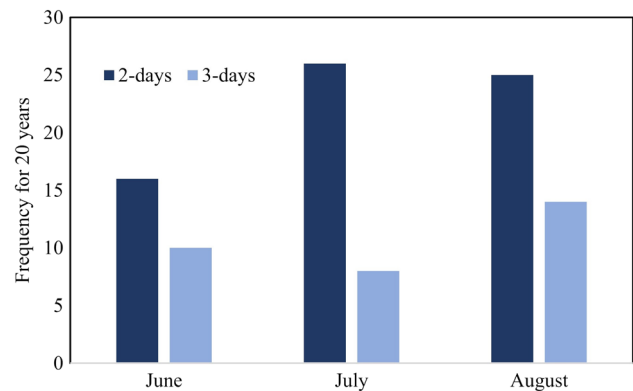


Fig. 7 Frequency of events for 20 years (2000–2019) where similar rainfall intensity (\pm mm/day) sustained for 2 and 3 consecutive days in the monsoon months (June–August)

areas (factor of safety) for only earthquake induced events are assessed for 50, 75, 100, 200, and 475 years.

The increase in landslide-prone areas under higher return periods is found for both cases (earthquake-rainfall-induced and only earthquake-induced landslide). Areas with higher slope values are found to be vulnerable, even for the lower return period combinations as well. Areas with lower soil depth have more landslide-prone areas. Camp 20 and Camp 20 extension have the higher amount of slide-prone areas followed by camp 17 and 18 (Figs. 8, 9).

Duration of rainfall has the most important impact in defining landslide-prone areas. More areas can be affected by greater rainfall duration in lower return periods compared to lower duration in higher return periods. However, PGA exceedance in longer return periods has specific significance. Therefore, the landslide-prone areas are assessed in longer return periods as well, and these return periods have the more vulnerable areas compared to the lower ones. Vulnerable areas increase in Camp 20, 20 extension and 17 with increased rainfall duration and return periods. Camp 8E, 8W and 18 also become equally vulnerable with the increase of return periods.

In the case of only earthquake-triggered landslides, changes in the amount of landslide-prone areas were also found. The study identified the highest amount of landslide-prone areas for the return period of 475 years. Comparing the earthquake-rainfall induced and only earthquake induced events, it is evident that rainfall plays a major role in decreasing factor of safety significantly.

Both the methods (Monte-Carlo simulation and direct estimation) show almost similar results for the return period combinations, with only 1% greater landslide-prone areas under the Monte-Carlo simulation method in most of the cases (Table 3).

The models are validated against the landslide inventory of 120 records prepared from field observation. The receiver operating characteristic (ROC) curve is prepared to validate the accuracy, where the area under the Curve (AUC) determines the accuracy. The accuracy was tested for 90%

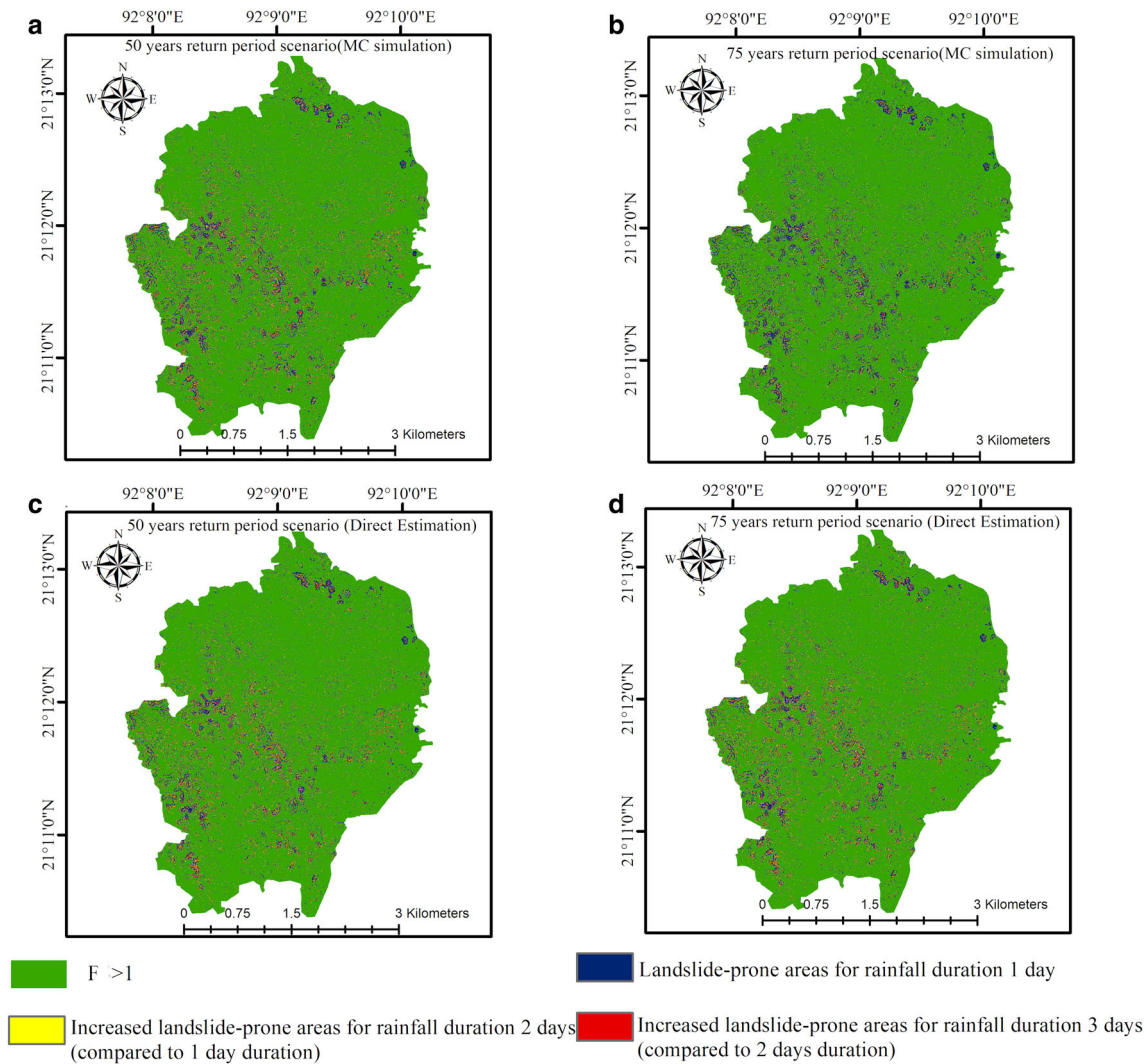


Fig. 8 Landslide-prone areas (factor of safety < 1) modelled for 1, 2, and 3 days of rainfall duration in Monte-Carlo simulation estimation method. **a** for 50 years return period, **b** for 75 years return period, and

in direct estimation method for, **c** for 50 years return period, **d** for 75 years return period

confidence intervals at different combinations. Each time the model showed more than 84% accuracy (Table 4).

4 Conclusion and recommendation

The main purpose of this study is to assess the landslide scenario, paying particular interest to identify the combined or sequential impact of earthquake and rainfall on landslide-prone areas. Therefore, the landslide-prone area of the Kutupalong Rohingya camp was identified as the site of the study. Three types of parameters (topographic parameters, soil physical property parameters, and contributing factors) have been combined to estimate the factor of safety in two different methods (Monte-Carlo simulation and direct estimation). To compensate for the uncertainties,

soil physical property parameters were designed employing two approaches: normal distribution (mean, standard deviation) and interpolation (IDW) for the Monte-Carlo simulation and direct estimation, respectively. Both estimations identified almost the same camp areas susceptible to failure, where the Monte-Carlo simulation has found 1% more vulnerable areas than the direct estimation method.

The contributing factors, earthquake PGAs for 50, 75, 100, 200, and 475 years return periods and rainfall intensity for 50 and 75 years were considered to estimate the factor of safety. Moreover, the effects of the duration of specific intensity rainfall have also been modeled. The study finds more areas vulnerable to slide with an increased value of PGAs and rainfall intensities, corresponding to an increased return period. Even for the same PGAs and rainfall intensity, areas with a factor of safety of less than 1

Fig. 9 Landslide-prone areas (factor of safety < 1) modelled for only earthquake-triggered landslide events for different return periods: **a** In Monte-Carlo simulation, **b** in direct estimation method

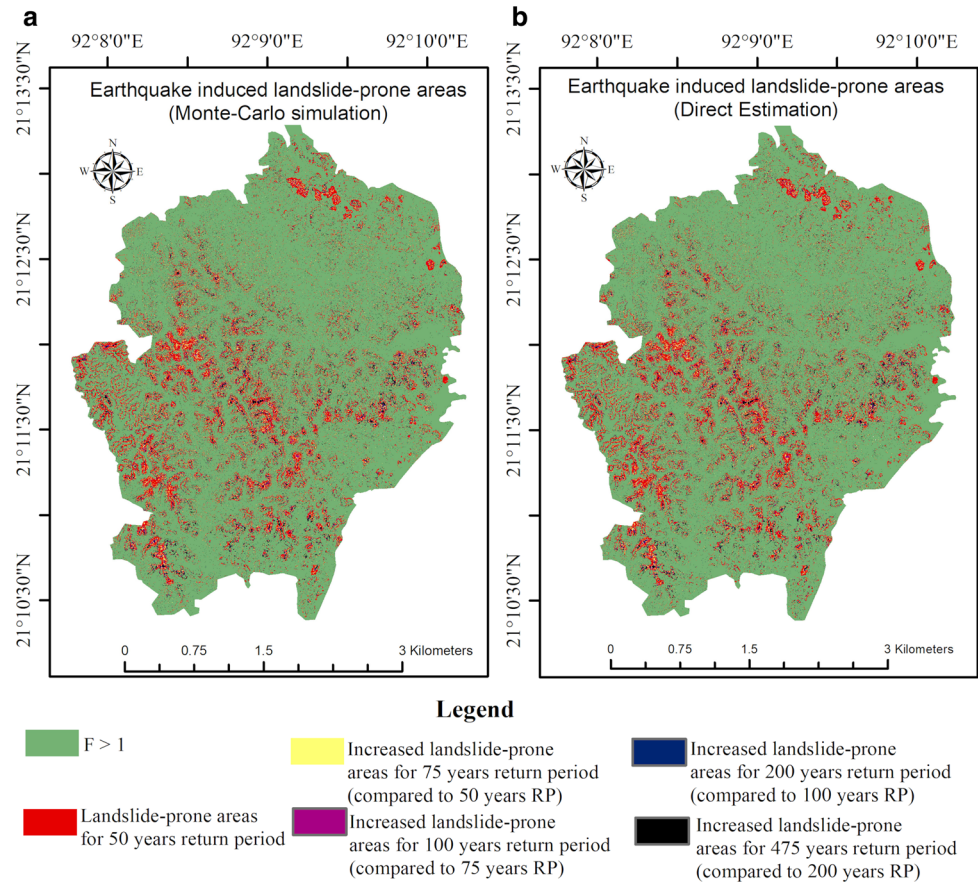


Table 3 Percentages of vulnerable areas estimated with specific PGA and rainfall intensity for different return period scenarios and duration of that specific rainfall combination

Return period (years)	Monte-Carlo simulation				Direct estimation			
	Earthquake-rainfall-induced landslide-prone areas			Earthquake-induced landslide-prone areas (%)	Earthquake-rainfall-induced landslide-prone areas			Earthquake-induced landslide-prone areas (%)
	1 Day	2 Day	3 Day		1 Day	2 Day	3 Day	
50	12	14	15	9	11	14	14	8
75	12	15	17	11	11	14	15	10
100	–	–	–	14	–	–	–	13
200	–	–	–	17	–	–	–	16
475	–	–	–	19	–	–	–	18

increased with the increase in rainfall duration. However, there lies some uncertainty regarding the rainfall intensity value at higher return periods, as rainfall parameters can be attributed to climate change issues. Therefore, the study has assessed the hazard scenario at 50 and 75 years return period scenario for earthquake-rainfall-induced scenario. Due to the significance of higher return periods in case of earthquake PGA exceedance, up to 475 years return period, which is equivalent to the PGA of 10% probability of exceedance in 50 years (Design-Based Earthquake, DBE),

the factor of safety has been calculated for earthquake-triggered events only.

Camp no. 17, 20, and 20-extension were found to have a significant amount of vulnerable areas at all the hazard scenario combinations owing to their curvature pattern (more convex or concave planes compared to other camps). Areas with higher slope values were found to be more prone to landslide than the lower slopes, where the slopes have planar surfaces.

This can be mentioned that the study area has undergone limited geological investigation till now as the camp has

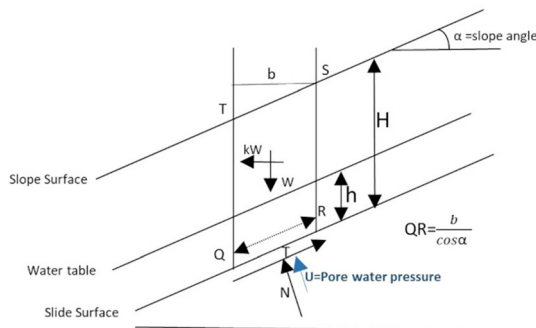
Table 4 Validation result at 90% confidence interval

Test result variable(s)	Area AUC	Std. error	Asymptotic 90% confidence interval	
			Lower bound	Upper bound
Return period 50 years	0.907	0.037	0.845	0.968
Return period 75 years	0.907	0.037	0.845	0.968
Return period 100 years	0.904	0.037	0.845	0.968
Return period 200 years	0.911	0.037	0.851	0.973
Return period 475 years	0.915	0.034	0.857	0.977

only been set recently. A more detailed geological investigation may feed the parameters more accurately. In fact, there is a scope to examine the risk of hazards in a more updated manner employing the parameters. Another important fact is the camp area’s dynamic nature. The Rohingyas are still cutting the slopes as per their convenience; more and more development activities have continuously been carried out, reshaping the camp area’s structure. This anthropogenic intervention is contributing to the landslide. Therefore, the most updated current topographic scenario can increase the accuracy of the landslide hazard assessment.

The study has executed a validation test using the landslide inventory of previously occurred ones, showing that the ROC curves possess AUC values ranging from 85 to 93% for all the assessed scenarios at different confidence levels. The study’s findings can be adopted for risk-sensitive land-use planning of the camp area. The area’s susceptibility to slides should be addressed, and proper mitigation measures must be adopted to improve the condition of the vast Rohingya community.

Appendix 1



The weight of the block QRST:

$$w = \gamma bH \tag{8}$$

where, γ = unit weight of soil, H = Thickness of soil.
 Height of water table above failure surface = h

$$\text{Weight of water} = w_w = \gamma_w bh \tag{9}$$

[γ_w is the density of water].

$$\text{Normal component of water weight, } P_w = \gamma_w bh \cos \alpha$$

$$\text{Pore pressure on QR, } u = \frac{P_w}{QR} = \frac{\gamma_w bh \cos \alpha}{\frac{b}{\cos \alpha}} = \gamma_w h \cos^2 \alpha \tag{10}$$

Earthquake loading is expressed as k_w , where seismic coefficient, k is multiplied by soil weight w which is working on the horizontal direction.

Forces perpendicular to slip plane:

$$N = W \cos \alpha - kW \sin \alpha$$

$$N = \gamma b H \cos \alpha - k \gamma b H \sin \alpha \quad [\text{From(8)}]$$

Forces parallel to the slip plane:

$$T = W \sin \alpha + kW \cos \alpha$$

$$T = \gamma b H \sin \alpha + k \gamma b H \cos \alpha \quad [\text{From(8)}]$$

$$\text{Shear stress, } \tau = \frac{T}{QR} = \frac{\gamma b H \sin \alpha + k \gamma b H \cos \alpha}{\frac{b}{\cos \alpha}} = \gamma H \sin \alpha \cos \alpha + k \gamma H \cos^2 \alpha \tag{11}$$

$$\text{Normal stress, } \sigma_n = \frac{N}{QR} = \frac{\gamma b H \cos \alpha - k \gamma b H \sin \alpha}{\frac{b}{\cos \alpha}} = \gamma H \cos^2 \alpha - k \gamma H \sin \alpha \cos \alpha \tag{12}$$

$$\begin{aligned} \text{Factor of Safety, } F_{Sp} &= \frac{\text{Resisting Force}}{\text{Driving force}} = \frac{c + (\sigma_n - u) \tan \theta}{\tau} \\ &= \frac{c + (\gamma H \cos^2 \alpha - k \gamma H \sin \alpha \cos \alpha - \gamma_w h \cos^2 \alpha) \tan \theta}{\gamma H \sin \alpha \cos \alpha + k \gamma H \cos^2 \alpha} \\ &= \frac{c + (\gamma H - \gamma_w h) \cos^2 \alpha \tan \theta - k \gamma H \sin \alpha \cos \alpha \tan \theta}{\gamma H \sin \alpha \cos \alpha + k \gamma H \cos^2 \alpha} \end{aligned}$$

Author contributions All authors contributed to the study conception and design. Material preparation, data collection and analysis were performed by AS-A, ASMMK, and MZR. The first draft of the manuscript was written by AS-A, and all authors commented on previous versions of the manuscript. All authors read and approved the final manuscript.

Funding Author Anika Samm-A received the National Science and Technology Fellowship from Ministry of Science and Technology, Bangladesh for this study.

Declarations

Conflict of interest The authors declare no competing interest.

References

- Ahmed B (2015) Landslide susceptibility modelling applying user-defined weighting and data-driven statistical techniques in Cox's Bazar Municipality, Bangladesh. *Nat Hazards* 79:1707–1737. <https://doi.org/10.1007/s11069-015-1922-4>
- Ahmed B, Rahman MS, Sammonds P et al (2020) Application of geospatial technologies in developing a dynamic landslide early warning system in a humanitarian context: the Rohingya refugee crisis in Cox's Bazar, Bangladesh. *Geomat Nat Hazards Risk* 11:446–468. <https://doi.org/10.1080/19475705.2020.1730988>
- Aristizábal E, García EF, Marin RJ et al (2020) Rainfall-intensity effect on landslide hazard assessment due to climate change in north-western Colombian Andes. *Rev Fac Ing Univ Antioquia*. <https://doi.org/10.17533/UDEA.REDIN.20201215>
- Aziz A (2021) 4 children among 8 killed in Cox's Bazar landslides. Dhaka Trib
- Blaser L, Krüger F, Ohrnberger M, Scherbaum F (2010) Scaling relations of earthquake source parameter estimates with special focus on subduction environment. *Bull Seismol Soc Am* 100:2914–2926. <https://doi.org/10.1785/0120100111>
- BMD (2021) Bangladesh Meteorological Department. <http://live4.bmd.gov.bd/>. Accessed 25 Dec 2021
- BNBC (2020) Bangladesh National Building Code (BNBC) 2020. House Build Res Inst
- Borga M, Dalla Fontana G, Cazorzi F (2002) Analysis of topographic and climatic control on rainfall-triggered shallow landsliding using a quasi-dynamic wetness index. *J Hydrol* 268:56–71. [https://doi.org/10.1016/S0022-1694\(02\)00118-X](https://doi.org/10.1016/S0022-1694(02)00118-X)
- Chisty KU (2014) Landslide in Chittagong City: a perspective on hill cutting. *J Bangladesh Inst Plan* 7:1–17
- Chow VT (1964) Handbook of applied hydrology. McGraw-Hill Book Company, New York
- Cunnane C (1978) Unbiased plotting positions—a review. *J Hydrol* 37:205–222. [https://doi.org/10.1016/0022-1694\(78\)90017-3](https://doi.org/10.1016/0022-1694(78)90017-3)
- Du W, Wang G (2014) Fully probabilistic seismic displacement analysis of spatially distributed slopes using spatially correlated vector intensity measures. *Earthq Eng Struct Dyn* 43:661–679. <https://doi.org/10.1002/EQE.2365>
- ESRI (2021) Curvature function—ArcGIS for Desktop. <https://desktop.arcgis.com/en/arcmap/10.3/manage-data/raster-and-images/curvature-function.htm>. Accessed 25 Dec 2021
- Factor Geotechnical (2021) What does friction angle of soil mean? <https://factorgeo.com/what-does-friction-angle-of-soil-mean/>. Accessed 25 Dec 2021
- Giiespie M (2021) Kutupalong Chronicles: floods and landslides. In: Chronicles from margins. <https://cov19chronicles.com/kutupalong-chronicles-floods-and-landslides-kill-6-rohingya-refugees-and-leave-5-million-homeless-in-coxs-bazaar-bangladesh/>. Accessed 25 Dec 2021
- Haneberg WC (2004) A rational probabilistic method for spatially distributed landslide hazard assessment. *Environ Eng Geosci* X:27–43
- Haque DME, Kamal DASMM, Rahman A, Bhuiyan MHF (2018) Landslide risk information for KTP Rohingya Refugee camp in Bangladesh. Am Geophys Union, Fall Meet 2018, Abstr #NH52B-10 2018:NH52B-10
- Harleman DRF, Mehlhorn PF, Rumer Jr RR (1963) Dispersion-permeability correlation in porous media. *J Hydraul Div* 89:67–85. <https://doi.org/10.1061/JYCEAJ.0000863>
- Hossain ATMS, Toll DG (2020) Rainfall induced landslide hazards of Bangladesh: challenges, issues and sustainable development. *Int J Sci Eng Res* 11:225–230
- Hynes Griffin ME, Franklin AG (1984) Rationalizing the seismic coefficient method. Final Report, Miscellaneous Paper No. GL-84-3, U.S. Army Engineer Waterways Experiment Station, Vicksburg, Mississippi
- Iida T (1984) A hydrological method of estimation of the topographic effect on the saturated throughflow. *Jpn Geomorph Union Trans* 5:1–12
- ISCG (2018) Risk on flood and landslide for Kutupalong RCI Humanitarian Response. In: Humanit. Serv. OCHA. <https://www.humanitarianresponse.info/ru/operations/bangladesh/infographic/risk-flood-and-landslide-kutupalong-rc>. Accessed 25 Dec 2021
- Jibson RW (2011) Methods for assessing the stability of slopes during earthquakes—a retrospective. *Eng Geol* 122:43–50. <https://doi.org/10.1016/j.enggeo.2010.09.017>
- Kamal ASMM (2013) Earthquake risk and reduction approaches in Bangladesh. In: Shaw R et al (ed) Disaster risk reduction approaches in Bangladesh. Japan, pp 103–130
- Kramer SL (1996) Geotechnical earthquake engineering, 1st edn. Prentice Hall, Hoboken
- Marcuson W (1981) Session 7: moderator's report. In: International conference on recent advances in geotechnical earthquake engineering and soil dynamics
- McClymont A, Bauman P, Miazga C et al (2017) Emergency response groundwater exploration at Rohingya refugee camps in Bangladesh. *Can J Explor Geophys* 43:12–18
- Nguyen VBQ, Kim YT (2020) Rainfall-earthquake-induced landslide hazard prediction by Monte Carlo simulation: a case study of MT. Umyeon in Korea. *KSCE J Civ Eng* 24:73–86. <https://doi.org/10.1007/s12205-020-0963-8>
- Reliefweb (2018) Rohingya influx overview: key changes during 2018 monsoon season—BangladeshReliefWeb. Cox's Bazar
- Reliefweb (2019) Bangladesh: rohingya face monsoon floods, landslides—BangladeshReliefWeb. In: OCHA Serv. <https://reliefweb.int/report/bangladesh/bangladesh-rohingya-face-monsoon-floods-landslides>. Accessed 25 Dec 2021
- Saulnier GM, Beven K, Obed C (1997) Including spatially variable effective soil depths in TOPMODEL. *J Hydrol* 202:158–172. [https://doi.org/10.1016/S0022-1694\(97\)00059-0](https://doi.org/10.1016/S0022-1694(97)00059-0)
- Seda Ç (2020) Effect of the slope angle and its classification on landslide. *Nat Hazards Earth Syst Sci*. <https://doi.org/10.5194/nhess-2020-87>
- Seed HB (1979) Considerations in the earthquake-resistant earth and rockfill dams. *Gebtechnique* 29(29):215–263
- Tehrani FS, Hüskén L (2019) Landslide susceptibility mapping of refugee camps in Bangladesh. In: 2nd international conference on natural hazards and infrastructure
- Terzaghi K (1950) Mechanism of landslides. *Appl Geol Eng Pract*. <https://doi.org/10.1130/BERKEY.1950.83>
- Terzaghi RD, Voight B (1979) Karl terzaghi on rockslides: the perspective of a half-century. *Dev Geotech Eng* 14:111–134. <https://doi.org/10.1016/B978-0-444-41508-0.50010-7>
- UNHCR (2021) Situation refugee response in Bangladesh. https://data2.unhcr.org/en/situations/myanmar_refugees. Accessed 4 Jan 2022
- Wang Y, Kerry S (2013) Active tectonic features that pose a seismic threat to Bangladesh. Report of Comprehensive Disaster Management Programme (CDMP)
- Wang Y, Sieh K, Tun ST et al (2014) Active tectonic and earthquake Myanmar region. *J Geophys Res Solid Earth* 119:3576–3822. <https://doi.org/10.1002/2013JB010762>. Received
- Wang JP, François B, Lambert P (2017) Equations for hydraulic conductivity estimation from particle size distribution: a

dimensional analysis. *Water Resour Res* 53:8127–8134. <https://doi.org/10.1002/2017WR020888>

Wells DL, Coppersmith KJ (1994) New empirical relationships among magnitude, rupture length, rupture width, rupture area, and surface displacement. *Bull Seismol Soc Am* 84:974–1002

Zhang Y (2015) Stability and run-out analysis of earthquake-induced Landslides. *Earthq Eng - From Eng Seismol to Optim Seism Des Eng Struct*. <https://doi.org/10.5772/59439>

Publisher's Note Springer Nature remains neutral with regard to jurisdictional claims in published maps and institutional affiliations.

Springer Nature or its licensor (e.g. a society or other partner) holds exclusive rights to this article under a publishing agreement with the author(s) or other rightsholder(s); author self-archiving of the accepted manuscript version of this article is solely governed by the terms of such publishing agreement and applicable law.